Egypt. J. Chem. **Vol. 67**, No. 7. pp. 221 - 232 (2024)

Egyptian Journal of Chemistry

http://ejchem.journals.ekb.eg/

Multiple Applications of Synthesized Hyperbranched Poly(Amidoamine)Dendrimer and Its Znonanohybrid: Anti-Microbial Agents, Anti-Biofilms, Biocides And Corrosion Inhibitors

W. Mahdy[a], K.I. Kabel[b], E.H El-Shatoury [c], A.M. Saeed [c], A. Labena [b]*

[a] *WASCO Petroleum Company, Cairo, Egypt.*

[b] *Egyptian Petroleum Research Institute (EPRI), Nasr City, Cairo, Egypt.*

[c] *Ain Shams University, Faculty of Science, Microbiology Department, Cairo, Egypt.*

Abstract

This study aimed to synthesize a hyperbranched poly(amidoamine) dendrimer (PAMAMD) and its ZnOnanohybrid (PAMAMD-Zn). The synthesized products were characterized using various techniques; XRD, DLS, SEM and FT-IR. Subsequently, the synthesized products were tested for their broad-spectrum antimicrobial activities. Additionally, they were evaluated for their suitability as biocides and corrosion inhibitors against aerobic and anaerobic corrosive bacteria which isolated from an Egyptian petroleum company's environment. The results were notably intriguing as both the synthesized products, PAMAMD and PAMAMD-Zn, demonstrated a broad-spectrum antimicrobial activity against various standard microbial strains. Furthermore, the PAMAMD-Zn exhibited a higher broad-spectrum antimicrobial activity with the lowest minimum inhibitory concentration (MIC), minimum bactericidal and fungicidal concentration (MBC, MFC) values compared to the PAMAMD. In addition, both products exhibited metal corrosion inhibition efficiencies against aerobic corrosive communities of 92.1 and 94.4%, respectively and anaerobic corrosive communities of 91.6 and 96.3%, respectively.

Keywords: Metal corrosion; Aerobic corrosion; Anaerobic corrosion; Poly(amidoamine)dendrimer; ZnO nanohybrid.

1. Introduction

Petroleum sectors around the world suffer from severe metal corrosion problems caused by various corrosive environments, often in conjunction with diverse microbial communities [1, 2]. Metal corrosion results in a multitude of economic, environmental, and safety issues [3]. Many of the metal corrosion problems in the petroleum sector are associated withmicro-organisms in a process known as microbially influenced corrosion (MIC) or biocorrosion [4]. Various microbial diversities have frequently been detected in petroleum pipelines and tanks, leading to MIC problems [5]. Well-known microbial communities reputedly associated with MIC problems include sulfate-reducing bacteria (SRB), iron-reducing bacteria (IRB), iron-oxidizing bacteria (IOB), acid-producing bacteria (APB), manganese-oxidizing bacteria (MOB), and slime-forming bacteria (SFB) [6-9]. Despite the routine application of desired metal-corrosion inhibitors and biocides, various microbial diversities inhabit the utilities within the petroleum sector. Therefore, the attention of researchers has been drawn towards designing novel products with multifunctional applications and specific desired characteristics. These products should have the ability to protect metal surfaces from corrosive media effectively, possess numerous functional groups, and be effective at low concentrations [10]. Among these materials, hyperbranchedpolyamidoamine (PAMAM)

*Corresponding author e-mail: a.labena@epri.sci.eg.; (Ahmed Labena).
EJCHEM use only: Received date 19 November 2023; revised date 30 December 2023; accepted date 14 January 2024
DOI: 10.21608/EJCHEM.2024.249866.8893

dendrimers have garnered significant attention due to their well-defined structure, excellent bio-compatibility, and versatile functionalization capabilities [11]. PAMAM dendrimers exhibit a three-dimensional, tree-like macromolecular structure with a core and multiple branches, resulting in a high degree of branching and molecular complexity. They are synthesized through a stepwise iterative process, allowing for precise control over their size, surface functionality, and internal voids, a method often referred to as 'one-pot synthesis. Furthermore, PAMAM dendrimers offer a multitude of terminal groups, making them an attractive option for hosting other molecules or nanoparticles [12]. It has been reported that PAMAMs have been applied as biocides and metal corrosion inhibitors to protect metal surfaces from microbial activity and corrosive media, respectively [13, 14]. Simultaneously, nanoparticles of Zinc oxide (ZnO) have emerged as highly promising candidates for a range of biological purposes. This is primarily due to their compatibility with living organisms, low toxicity, and potential antimicrobial properties [15]. ZnO functions as a wide-bandgap semiconductor with exceptional optoelectronic characteristics, making it a sought-after material in various applications. In recent times, increasing attention has been directed towards its potential biological functions, including its ability to combat bacteria and potentially assist in cancer treatment. ZnO's biocompatibility and its capacity to generate reactive oxygen species (ROS) upon exposure to ultraviolet (UV) light contribute to its appeal as a compelling option in the realm of biomedical applications [16]. By combining the advantageous features of the PAMAM dendrimers with nanoparticles, researchers have created hybrid-nanocomposites with enhanced biological activity, opening up exciting possibilities for many industrial applications. [17-20].To harness the benefits of the PAMAM and nanoparticles, researchers successfully developed novel PAMAM nanocomposites to be used in diverse industrial applications [21-24]. Therefore, this study directed to synthesis of hyperbranched poly(amido-amine) dendrimer (PAMAMD) and its decorated nano Zinc form, hyperbranched poly(amidoamine)dendrimer/ZnOnanohybrid (PAMAMD-Zn). These synthesized products were comprehensively characterized using techniques including X-ray Diffraction (XRD), Dynamic Light Scattering (DLS), Scanning Electron Microscopy (SEM) and Fourier Transform Infrared (FT-IR). They were then tested to evaluate their broad-spectrum antimicrobial activity against various standard microbial strains, with the determination of minimum inhibitory concentrations and minimum bactericidal/ fungicidal concentrations (MBC/MFC). Furthermore, their effectiveness as biocides and metal corrosion inhibitors was assessed against environmental aerobic and anaerobic bacterial communities, previously isolated from a natural gas company with a salinity of 23,000 ppm (NaCl concentration).

2. Materials and method

2.1. Chemicals

Methyl acrylate, ethylene diamine, 1,1,1-trimethylolpropane (TMP), p-toluene sulphonic acid (PTSA), Ethanol, Zinc sulphate, Sodium hydroxide and Glycidoxypropyltrimethoxysilane (GPTMS) were supplied from Sigma Aldrich.

2.2. Synthesis of hyperbranched poly(amidoamine) dendrimer (PAMAMD)

The AB2 monomer of hyperbranched poly(amine-ester) was synthesized through the reaction of 1 mol of methyl acrylate and 1 mol of ethylene diamine at 35 ^{o}C under continuous stirring for 4 h. This reaction was established in the presence of ethanol as a solvent and under nitrogen atmosphere. Subsequently, 1 mole of the core TMP was subjected to a reaction with 9 moles of the produced AB2 monomer after purification (using a rotary evaporator at 40 0C with a reduced pressure to obtain the final product). This reaction occurred with 0.5 wt % PTSA as a catalyst, THF as a solvent, and was maintained at a temperature of 120°C with constant agitation for a duration of 3 h. The end result was the creation of a hyperbranched polymer featuring amine terminals [13].

2.3. Synthesis of ZnO nanoparticles

ZnO nanoparticles were synthesized referring to [25]. Briefly, a Zinc precursor solution was prepared by dissolving 0.5 M of Zinc sulfate ($ZnSO_4$) in 100 ml of ethanol. The addition of sodium hydroxide served as the catalyst to initiate the reaction. Subsequently, the solution underwent 30 min of sonication to ensure the full formation of $Zn(OH)_2$. Afterward, the solution was collected via centrifugation and subjected to multiple washes with ethanol to eliminate impurities

then dried at 80 °C for 4 h, finally the dried powder was calcinated at 400°C for 2 h. The resulting ZnO nanoparticles were provided.

2.4.Synthesis of hyperbranched poly(amido-amine) dendrimer-ZnOnanohybrid (PAMAMD-Zn)

Approximately 100 mg of ZnO nanoparticles were initially dispersed in 10 ml of ethanol through ultrasonication for a period of 10 min. To this solution, 100 mg of Glycidoxypropyltrimethoxysilane (GPTMS) was introduced. The mixture underwent further ultrasonication for 3 h to facilitate the reaction. Any unreacted GPTMS was subsequently separated through a centrifugation. The resulting precipitate, composed of GPTMS-modified ZnO nanoparticles, was rinsed three times with ethanol to ensure complete elimination of any residual unreacted GPTMS. Following this, approximately 100 mg of the surface-modified ZnO nanoparticles were dispersed in 20 ml of ethanol. Then, 10 ml of the synthesized PAMAMD was added to the mixture. This combination, GPTMS-modified ZnO nanoparticles and PAMAMD, was stirred at 50°C for 6 h. Upon completion of the reaction, the chemically modified PAMAMD-ZnOnano-composite was once again collected through centrifugation. Finally, the collected nanocomposite material was air-dried for one day to eliminate any remaining solvents, resulting in the formation of the PAMAMD-Zn nanocomposite [26]. **Scheme 1** displayed the preparation steps of the synthesized materials.

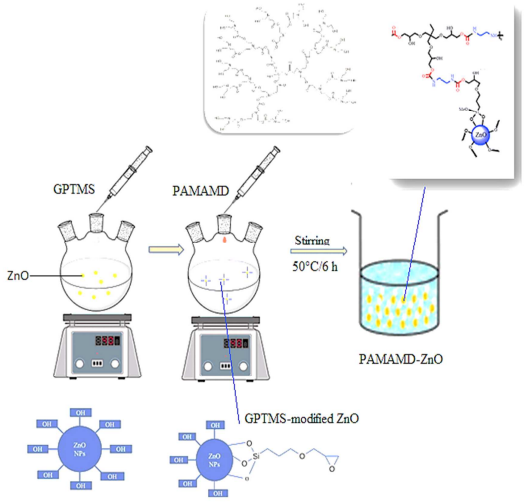

Scheme 1: The preparation steps of the synthesized materials

2.5. Characterization techniques

The crystalline structure of the synthesized nanoparticles was confirmed using "X-ray Diffraction (XRD) using the X-Pert Pro model, operating under specific conditions of 40 mA, 40 kV, and with Copper Kα1 radiation at a wavelength of 1.54 Å, employing a Cu-Kα radiation (λ = 1.5406 Å) Diffractometer". To determine the distribution of particle sizes, Dynamic Light Scattering (DLS) was applied, employing "a laser angle of 90° at a temperature of 25°C, utilizing the Zetasizer Nano-ZS90 instrument by Malvern Co., UK". Additionally, the physical structure and morphology of the prepared materials were investigated using Scanning Electron Microscopy (SEM), which was carried out with "a JEOL JEM-2100F microscope operating at 200 KV, manufactured in Japan". Furthermore, the prepared materials were subjected to various analyses to understand their composition and properties. "A Nicolet iS10 FT-IR spectrophotometer (Thermo-Fisher Scientific, USA)" was used to examine their chemical composition and functional groups across a wavenumber range spanning from 500 to 4000 cm^{-1}.

2.6. Application of the synthesized inhibitors as broad-spectrum antimicrobial agents

2.6.1. Microbial media

Bacterial media: Mueller Hinton agar (MHA) and broth (MHB) ("Difco, Franklin Lakes, NJ, USA"), Candida media: Sabouraud Dextrose Agar (SDA) and Broth (SDB) ("Difco, Sparks, MD, USA").

2.6.2. Standard microbial strains

Bacillus subtilis(ATCC 6633), abbreviated as *B. subtilis,*
Escherichia coli(ATCC 8739), abbreviated as *E. coli,*
Candida albicans(IMRU3669), abbreviated as *C. albicans.*

2.6.3. Biological susceptibility

The biological susceptibility of the synthesized inhibitors, namely the hyperbranched poly(amido-amine) dendrimer (PAMAMD) and the hyperbranched poly(amidoamine) dendrimer-ZnOnanohybrid (PAMAMD-Zn), both at a starting concentration of 1000 ppm, was evaluated using the agar well diffusion method, as described previously [27]. This assessment was conducted against bacterial and Candida standard strains on MHA and

SDA, respectively. The procedure involved streaking the standard strains on their selective-media agar plates, followed by the creation of 10 mm wells on the surface using a sterile borer. Subsequently, 100 µl of PAMAMD and PAMAMD-Zn were added to each well. After an incubation period at 35°C, which lasted overnight for bacterial strains and 48 h for the Candida strain, the biological susceptibility was assessed by measuring the diameter of the clearing zone (in millimeters). This series of tests was conducted three times, and the average values were recorded. Sterile water served as a negative control, while standard antimicrobial agents were employed as positive controls.

2.6.4. Determination of Minimum inhibitory concentration (MIC), Minimum Bactericidal/Fungicidal Concentration (MBC/MFC) values

The Minimum inhibitory concentration (MIC) "is defined as the lowest concentration of an antimicrobial agent that inhibits the development of visible microbial growth" [28]. The MICs of the synthesized inhibitors were determined using a modified micro-dilution method in 96-well microtiter plates, as previously described [29]. The inoculation of bacterial and Candida strains followed the protocol outlined by the Clinical Laboratory Standards Institute (CLSI) [30, 31].

Initially, 100 µl of the synthesized inhibitors at an initial concentration of 1000 ppm were subjected to serial dilution, using MHB for bacterial strains and SDB for the Candida strain. This dilution process was carried out in "NunclonTMmicrotiter plates (Nunc GmbH & Co., Wiesbaden, Germany)".

The wells with serially diluted inhibitors were then inoculated with 100 µl of a microbial suspension containing 1-2x10^8 CFU/ml for Grampositive standard bacterial strains, 1-2x109 CFU/ml for Gram negative standard bacterial strains, and 5x10^6 CFU/ml for the standard Candida strain.

Concurrently, two control groups were included: a negative control consisting of sterile media only and a positive control consisting of media inoculated with microbes but without the synthesized inhibitors. Subsequently, the plates were placed in an incubator at 35°C for 20 h for the testing standard bacterial strains and for 72 h when assessing the Candida standard strain. To validate and observe the results, 30 µl of a 0.01% resazurin solution (HiMedia) was introduced into the wells [32], followed by an additional incubation period of 3 h. The change in color of the well to pink served as an indicator of a positive result. To determine the minimum bactericidal/fungicidal concentration (MBC/MFC) values of the synthesized inhibitors (PAMAMD and PAMAMD-Zn), 10 µl of the inhibitor was taken from the wells before adding resazurin that showing no observable microbial growth. These samples were then sub-cultured onto corresponding agar media (MHA for bacterial strains and SDA plates for Candida) [33]. The plates were subsequently incubated at 35°C for 20 h for standard bacterial strains and for 48 h for the Candida standard strain. The MBC/MFC was defined as "the lowest concentration of an antimicrobial agent required to kill 99% of the microorganisms" [34].

2.7. Application of the synthesized inhibitors as and biocides corrosion inhibitors

The aerobic and anerobic bacterial community in this study was enriched from a sample collected from the separator drain of El Wastani Petroleum Co. (WASCO), Wastani Field, Damietta City, Egypt named EW9. The field was suffered from severe corrosion problems although biocides and corrosion inhibitors are continuously applied. The enriched sample, under aerobic and anerobic conditions, was characterized by 16S metagenomics analysis. The aerobic bacterial community of the sample was mostly affiliated to two species *Pseudomonas* sp. and *Pseudomonasbalearica*. In addition, the anaerobic bacterial community of the collected sample was represented mostly by a species of *Desulfovibrioalaskensis*.

The synthesized inhibitors, namely PAMAMD and PAMAMD-Zn, were employed as biocides and corrosion inhibitors in the presence of both aerobic and anaerobic bacterial communities at a salinity level of 230,000 ppm (NaCl concentration). Corrosion was assessed using the weight loss method [35]. To conduct this evaluation, mild steel coupons with a chemical composition detailed in **Table 1** (AISI 1018 mild carbon steel strips measuring 1.5 x 1.5 x 0.32 cm, provided by COSASCO's Rohrback Systems, Inc) were utilized. These coupons were initially subjected to mechanical cleaning using emery papers of various grades and followed the cleaning procedure outlined in NACE Standard RP0775-99, Item No. 21017, and

were then thoroughly dried. The weight loss method involved comparing the weight of the coupons before and after the inhibition experiment. The corrosion rate of the metal (expressed in g/m2 per day) [36] and the inhibition efficiency (%) [37] were determined based on the weight loss results observed after one month of incubation. Duplicate experiments were conducted, and the average values along with the standard deviation of the calculated results were determined. For the inhibition experiments, a batch culture was prepared using a modified nutrient-rich simulated seawater (NRSS) medium [36] for the aerobic bacterial community and a modified Postgate's-C medium [38] for the anaerobic bacterial community. The modified NRSS and Postgate's-C media were formulated with a salinity of 23,000 ppm (NaCl concentration) and an initial pH of 6.8. During the media preparation process, these conditions were maintained. For the inhibition experiment, various concentrations of the synthesized inhibitors were used, including 500, 250, 125, and 62.5 ppm, alongside two control groups: the blank, which contained un-inoculated modified media, and the control, which was inoculated with either the aerobic or anaerobic bacterial community but without the synthesized inhibitors. The NRSS media were inoculated with an enriched aerobic bacterial community that had been previously cultivated for 20 h at 35°C. The bacterial count in the inoculum was estimated to be 5.2 x 10^5 CFU/ml based on total bacterial counts [39]. On the other hand, the inoculum for the anaerobic bacterial community contained 1.5 x 10^7 CFU/ml, and this count was determined using the most probable number (MPN) method with 3 tubes [40]. The preparation of the inoculum followed the modified Hungate's technique for anaerobic organisms [41].

Table 1. Chemical composition of a mild steal coupon

Element	Content
Carbon (C)	0.14 - 0.20 %
Iron (Fe)	98.81 - 99.26 %
Manganese (Mn)	0.60 - 0.90 %
Phosphorous (P)	≤ 0.040 %
Sulphur(S)	≤ 0.050 %

3. Results and discussion

3.1. Characterization techniques

The confirmation of the structural integrity across morphological attributes and particle size distributions of the synthesized material was assessed using XRD, SEM, and DLS techniques. The prepared hyperbranched polymer PAMAMD was clearly displayed in **Figure 1a**. where the main peaks were demonstrated within 2θ values 4, 15, and 22. The XRD patterns depicted in **Figure 1b**, were analyzed to determine the average particle size via the Debye-Scherrer equation (Equation 1):

$$D = 0.9\lambda/\beta\cos\theta \quad \ldots\ldots\ldots\ldots\ldots\ldots \quad (1)$$

where D represents crystal size, λ is the x-ray wavelength, β is the full width at half maximum of the diffraction peak, and θ is the Bragg diffraction angle. The observed data indicated that all peak values corresponded to the hexagonal structure of ZnO NPs, aligning with the JCPDS card (Card No. 89-1397). The high intensity and narrow width of ZnO diffraction peaks affirmed the resultant product's crystallinity, with a calculated average size of approximately 95 nm. **Figure 2** presented particle size distribution and PDI values for the prepared polymer nanocomposite which further supporting the homogeneity with high crystallinity of ZnO integrated in PMAM.

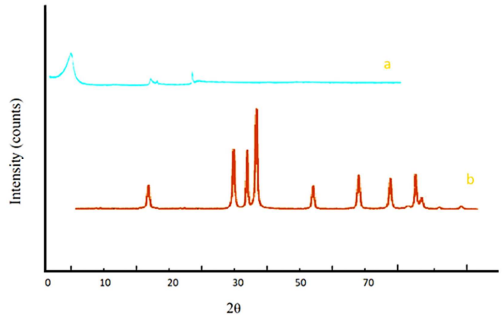

Figure 1: XRD patterns of the synthesized PAMAMD (a), and the PAMAMD-Zn (b)

Figure 2 exhibited the particle distribution of the prepared ZnO nanoparticles and the average particle size was 95 nm.

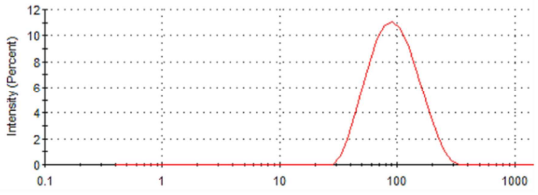

Figure 2: DLS of the prepared ZnO nanoparticles

Moreover, **Figure 3** displayed the SEM images of the prepared materials; a macroscopic view confirmed the homogenous structure of the prepared polymer and

the prepared nanocomposites. **Figure 3a**, showed the morphological structure of the PAMAM. Furthermore, **Figure 3b**, revealed the difference in the morphological structure of the prepared nano-composite than the pure polymer. In addition; it confirmed the dispersion and the well distribution of the ZnO nanoparticles within the PAMAMD matrix.

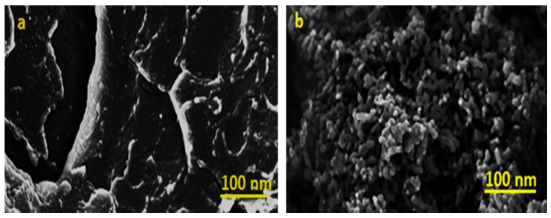

Figure 3: SEM images of the synthesized PAMAMD (a), and the PAMAMD-Zn (b)

To confirm the chemical structure of the prepared materials, FT-IR (Fourier Transform InfraRed) spectroscopy was carried out (see **Figure 4**). The spectrum corresponding to the PAMAMD (**Figure 4a**) clearly showed the distinguished bands of the polymer at 1650 cm^{-1} and 1532 cm^{-1} which related to CONH groups and a spike band at 3290 cm^{-1} that corresponded to NH_2 groups. New absorption bands at the stretching vibration area at 865 cm^{-1} and 710 cm^{-1} (**Figure 4b**) which clearly demonstrated the ZnO grafting on the polymer matrix.

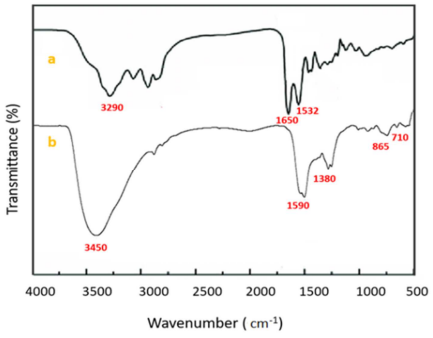

Figure 4: FT-IR spectra of the synthesized PAMAMD (a), and the PAMAMD-Zn (b)

3.2. Application of the synthesized inhibitors as broad-spectrum antimicrobial agents

Results, see **Table 2** and **Figure 5**, showed broad anti-microbial spectrum of the synthesized inhibitors against Gram positive (*B. subtilis*) and negative bacterial (*E. coli*) and Candida (*C. albicans*) standard strains. The PAMAMD displayed an anti-microbial activity with clearing zones of 27, 25.5 and 30.5 mm against *B. subtilis*, and *E. coli* and *C. albicans*, respectively. Moreover, the PAMAMD-Zn showed clearing zones of 33, 29 and 33 mm against *B. subtilis,* and *E. coli* and *C. albicans*, respectively which are higher than the PAMAMD values. This may attribute to the antimicrobial effect of Zinc nanoparticles as previously reported [16]. Moreover, the synthesized inhibitors have displayed anti-microbial activity against Gram positive (*B. subtilis*) bacterial strain with clearing zones of 27, 33 mm which are higher than against Gram negative (*E. coli*) bacterial strain with clearing zones of 25.5, 29 mm. This effect was mostly due to the changes in the cell-membrane of positive and negative Gram bacteria. It is well known that; Gram positive bacterial membrane is a single layer in comparison to bilayer membranes in Gram-negative bacterial membrane. The additional outer membrane layer provides the Gramnegative bacteria more resistant to an anti-microbial agent [42]. That means Gram positive bacterial strains are more sensitive to antimicrobial agents than Gram-negative bacteria [43]. In addition, the strength of the bacterial membrane disruption of the Gram-negative bacteria plays a crucial role in the resistivity action [44, 45].

Table 2. The antimicrobial activity of the synthesized inhibitors

Inhibitors	*Bacillus subtilis* (ATCC 6633)	*Escherichia coli* (ATCC 8739)	*Candida albicans* (IMRU3669)
	Inhibition zone (mm)		
PAMAMD	27 ± 1.0	25.5 ± 0.5	30.5 ± 0.5
PAMAMD-Zn	33.0 ± 1.0	29 ± 0.0	33 ± 0.0
*AMC (100 ppm)	19.5 ± 0.5		
*TE (100 ppm)		18 ± 0.0	
* Flu (100 ppm)			27 ± 0.0

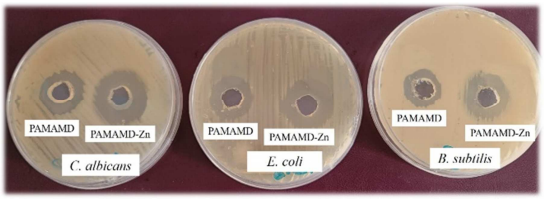

Figure 5: Photos display the antimicrobial activity of the synthesized inhibitors

Table 3 and **Figure 6**reported the "minimum inhibitory concentrations (MICs), minimum bactericidal concentrations (MBCs) and minimum fungicidal concentrations (MFCs) of the synthesized inhibitors. The synthesized inhibitors exhibited MICs/MBCs values of 31.25/31.25 ppm against Gram positive (*B. subtilis*) bacterial strain and values of 31.25–62.5/62.5–125 ppm against Gram negative (*E. coli*) bacterial strain. In addition, they displayed

MICs/MFCs against Candida (*C. albicans*) strain with values of 15.6/15.6–31.25 ppm. Moreover, the synthesized PAMAMD-Zn has demonstrated lower values in comparison to the synthesized PAMAMD counterpart. This behaviour was totally attributed to the effect of ZnO nano metals [46].

Scientist have severally reported the antimicrobial effect of the poly(amido-amine) dendrimers. They have a distinguish anti-microbial activity due to their highly functional, localized and branching groups in addition to their unique structure [47- 49].

The uniform branching of dendrimers increases their surface area and hence increases their biocidal reactivity [50]. Furthermore, the antibacterial effect of poly (amidoamine) dendrimers can be attributed to an electrostatic interaction between the anionic surface (phospholipid membrane) and the cationic charges of the poly (amidoamine) dendrimers.

This interaction ultimately results in a modification of the cell's permeability [51- 53] leading to subsequent disruption of the bacterial cell membrane and, consequently, bacterial cell death [54, 55]. Similarly, the antifungal activity of poly(amidoamine) dendrimers is linked to an electrostatic interaction between the negatively charged residues on the fungal cell surface and the positively charged poly(amidoamine) dendrimers.

This interaction causes a leakage of intracellular electrolytes [56, 57]. Additionally, it has been reported that dendrimers may interfere with fungal enzyme activities [58]. Zinc nanoparticles are well-known for their high biocompatibility, chemical stability, binding capabilities, and antimicrobial potential when used in conjunction with dendrimers [59].

When poly (amidoamine) dendrimers are hybrid with zinc nanoparticles, their antimicrobial effectiveness is enhanced. Zinc nanoparticles can generate reactive oxygen species, which can break down bacterial cells [60]. Furthermore, zinc nanoparticles can interact with the bacterial cell membrane, disrupting its integrity and ultimately leading to cell death [61].

Table 3. The MIC, MBC and MFC values of the synthesized inhibitors

Inhibitors	*Bacillus subtilis* (ATCC 6633)		*Escherichia coli* (ATCC 8739)		*Candia albicans* (ATCC 10231)	
	MIC	MBC	MIC	MBC	MIC	MFC
PAMAMD	31.25	31.25	62.5	125	15.62	31.25
PAMAMD-Zn	31.25	31.25	31.25	62.5	15.62	15.62

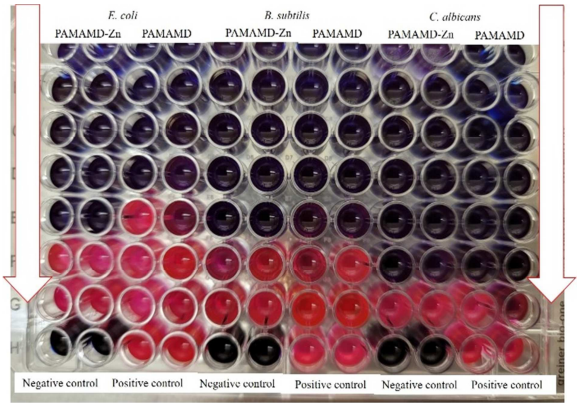

Figure 6: Photos demonstrating the MIC values detection of the synthesized inhibitors

3.3. Application of the synthesized inhibitors as and biocides corrosion inhibitors

In this work, the synthesized inhibitors were used in addition as biocides and corrosion inhibitors against both aerobic and anaerobic bacterial communities (see **Figure 7a, b**). The blank reactor corrosion rate (uninoculated modified NRSS media) was 3.874 ± 0.12 gm^2/d (**Figure 8**) which probably affiliated to the salinity media and particularly the chloride anion that increases the metal corrosivity. In addition, the chloride anion increases the aqueous media conductivity, damages the established passive film and subsequently induce pitting corrosion [62, 63]. Nevertheless, the control reactor corrosion rate (inoculated by aerobic microbial diversity without the synthesized inhibitors) was 2.86 ± 0.01 gm^2/d. This result was lower than for the blank reactor. This attitude may attribute to the activity of the corrosive aerobic bacterial community`s biofilm that covered the metal from the salinity attack [64- 67]. *Pseudomonas*sps, as aerobic slime-forming bacterial diversity, are the most predominate detected bacteria in marine environment that form biofilm and induce microbially influenced corrosion for metals. Once the biofilm develops on the metal surface, it initiates a chemical process within localized aeration cells [36]. This localized aeration cells lead to an activation of an electrotechnical-cell and afterwards induce a pitting metal corrosion [68, 69]. Furthermore, the presence of aerobic biofilm, particularly those forming slimy layers, can expedite metal corrosion through a catalyzed chemical reaction. This reaction occurs when the acidic extracellular polymeric substance (alginate) excreted by the biofilm interacts with the

metal surface, resulting in the formation of EPS-Fe(III) and subsequently triggering pitting corrosion [70, 71]. However, the introduction of the synthesized inhibitors (PAMAMD and PAMAMD-Zn) onto the metal surfaces led to a reduction in the corrosion rate as the concentrations of the synthesized inhibitors increased.

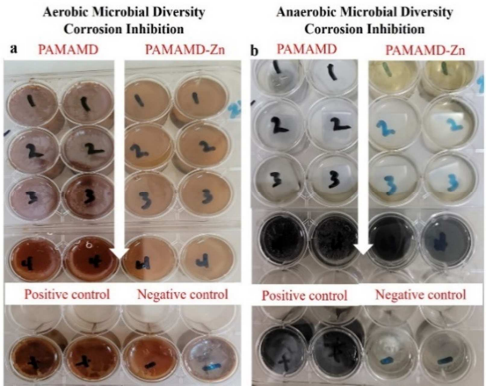

Figure 7: Photos documenting the anti-corrosion susceptibility of the synthesized PAMAMD, and the PAMAMD-Zn against aerobic microbial diversity (left) and anaerobic microbial diversity (right)

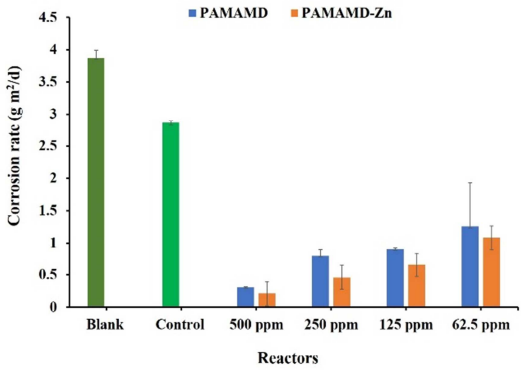

Figure 8: The metal corrosion rate of the synthesized PAMAMD, and the PAMAMD-Zn at different concentrations in addition to the blank and control reactors against aerobic microbial diversity

In the case of application of the synthesized inhibitors as a biocides and corrosion inhibitors against anaerobic bacterial community that cultivated at a medium salinity of 23000 ppm (NaCl concentration (see **Figure 9**). The metal corrosion rates under anaerobic condition were lower than under aerobic condition. The blank reactor corrosion rate (uninoculated modified Postgate`s C media) was 0.336 ± 0.02 gm^2/d. Neverthaless, the control reactor corrosion rate (inoculated by anaerobic microbial diversity without the synthesized inhibitors) was 0.516 ± 0.03 gm^2/d. This corrosion rate was higher than the blank reactor corrosion rate. This result was mainly attributed to the enriched anerobic microbial diversity which attached and induced sever metal corrosion. It has been reported that, there are many suggested mechanisms that SRB used to induce metal corrosion. The first attributed to the metabolites that they produced such as sulfide anion in all forms, dissolved, precipitated or evaporated [72]. The second suggested mechanism was correlated to the corrosion process which called cathodic depolarization [68, 69]. The third suggested mechanism was linked to the establishment of SRB biofilms on the metal surfaces [70]. A more recent fourth hypothesis was associated with the concept of extracellular electron transfer (EET) [73, 74].

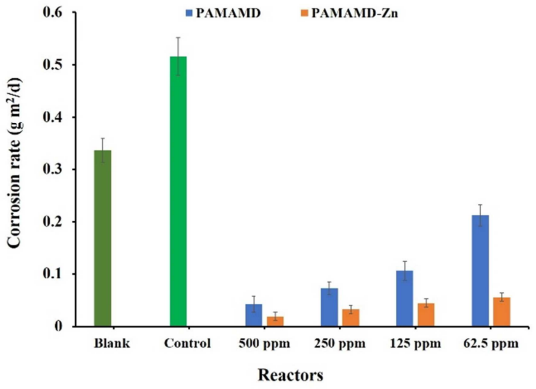

Figure 9: The metal corrosion rate of the synthesized PAMAMD, and the PAMAMD-Zn at different concentrations in addition to the blank and control reactors against anaerobic microbial diversity

The metal corrosion inhibition efficiencies against aerobic bacterial community were calculated from the corrosion rates (see **Figure 10**). The inhibition efficiency of 92.1% was attained when using 500 ppm of PAMAMD. However, by incorporating PAMAMD-Zn at the same concentration, the corrosion inhibition efficiency increased to 94.4% compared to PAMAMD alone. This enhancement in corrosion inhibition efficiency can be predominantly attributed to the presence of Zn nanoparticles within the PAMAMD [24, 75]. Similarly, the synthesized inhibitor PAMAMD has displayed a corrosion inhibition efficiency of 91.6 % lower than detected for the inhibitor PAMAM-Zn that was 96.3 % at a concentration of 500 ppm against anaerobic bacterial community that cultivated. The biocidal and the corrosion inhibition efficiencies of the synthesized PAMAMD was mainly attained to many factors. The

suggested antimicrobial capabilities of the synthesized inhibitors have been explained earlier. The metal corrosion inhibition was relied on many mechanisms. The first mechanism was correlated to its potentiality of chemisorption and hence a protected passive film will be established on the metal. Furthermore, the second suggested mechanism was linked to the binding capacity of the synthesized inhibitor with the metal surface. This interaction relies on the electronic charges or the active functional groups present in the synthesized inhibitors [76, 77].

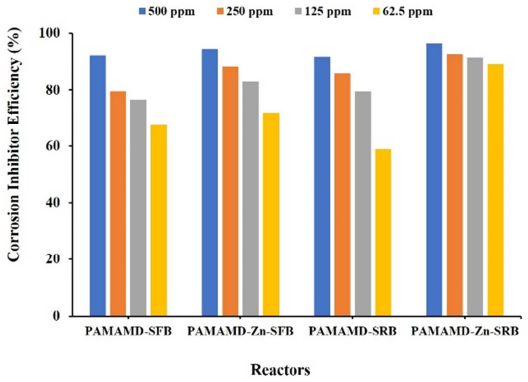

Figure 10: The corrosion inhibition efficiencies of the synthesized PAMAMD, and the PAMAMD-Zn against aerobic and anaerobic microbial diversity

4. Conclusion

Two synthesized products, hyperbranched poly(amidoamine)dendrimer (PAMAMD) and its ZnOnanohybrid (PAMAMD-Zn) have successfully synthesized and characterized using XRD, DLS, SEM and FT-IR. Afterwards. the synthesized products have exhibited extensive antimicrobial properties against both Gram-positive and Gram-negative bacteria, as well as Candida strains. Moreover, the PAMAMD-Zn have demonstrated better activities with higher inhibition zones and relatively lower MIC/MBC, MFC values in comparison to the synthesized PAMAMD. In addition, the synthesized products have successfully protected the metal surface from corrosiveness aerobic microbial diversity-induced corrosion-activity but also against anaerobic microbial diversity induced corrosion-activity. The results displayed that, the corrosion inhibition efficiencies of 92.1 and 94.4 % were achieved at a concentration of 500 ppm for the PAMAMD and PAMAMD-Zn, respectively against the aerobicmicrobial diversity-induced corrosion-activity. Similarly, at the same concentration, the highest corrosion inhibition efficiencies of 91.6 and 96.3 % for the PAMAMD and PAMAMD-Zn, respectively against the anaerobic microbial diversity-induced corrosion-activity.

Conflicts of interest: there no conflict of interest between the authors.

Formatting of funding sources: Science, Technology & Innovation Funding Authority (STDF) for funding the research project (ID: 38142)

Acknowledgment: Thanks for Science, Technology & Innovation Funding Authority (STDF) for funding the research project (ID: 38142).

References

[1] G.H. Koch, M.P. Brongers, N.G. Thompson, Y.P. Virmani, J.H. Payer, Corrosion cost and preventive strategies in the United States, United States. Federal Highway Administration, 2002, pp. 23–31.
[2] J. Guan, B.-L. Zhang, S.M. Mbadinga, J.-F. Liu, J.-D. Gu, B.-Z. Mu, Functional genes (dsr) approach reveals similar sulphidogenic prokaryotes diversity but different structure in saline waters from corroding high temperature petroleum reservoirs, Applied Microbiology and Biotechnology 98 (2014) 1871-1882.
[3] M. Lv, M. Du, X. Li, Y. Yue, X. Chen, Mechanism of microbiologically influenced corrosion of X65 steel in seawater containing sulfate-reducing bacteria and iron-oxidizing bacteria, Journal of Materials Research and Technology 8 (2019) 4066-4078.
[4] H.H. Almahamedh, C. Williamson, J.R. Spear, B. Mishra, D.L. Olson, Identification of microorganisms and their effects on corrosion of carbon steels pipelines, NACE CORROSION, NACE, 2011, pp. NACE-11231.
[5] A. Labena, M.A. Hegazy, H. Horn, E. Müller, Sulfidogenic-corrosion inhibitory effect of cationic monomeric and gemini surfactants: planktonic and sessile diversity, Royal Society of Chemistry Advances Journal 6(2016) 42263-42278.
[6] M.K. Pal, M. Lavanya, Microbial Influenced Corrosion: Understanding Bioadhesion and Biofilm Formation, Journal of Bio-and Tribo-Corrosion 8 (2022) 1-13.
[7] A. Marciales, Y. Peralta, T. Haile, T. Crosby, J. Wolodko, Mechanistic microbiologically influenced corrosion modeling—A review, Corrosion Science 146 (2019) 99-111.
[8] R. Jia, D. Yang, J. Xu, D. Xu, T. Gu, Microbiologically influenced corrosion of C1018 carbon steel by nitrate reducing *Pseudomonas aeruginosa* biofilm under organic carbon starvation, Corrosion Science 127 (2017) 1-9.
[9] D. Xu, Y. Li, T. Gu, Mechanistic modelling of biocorrosion caused by biofilms of sulfate reducing bacteria and acid producing bacteria, Bioelectrochemistry 110 (2016) 52-58.
[10] M. Chen, S. Zhou, B. You, L. Wu, A novel preparation method of raspberry-like PMMA/SiO2

hybrid microspheres, Macromolecules 38 (2005) 6411-6417.
[11] W. Ye, J.M. DeSimone, Emulsion polymerization of N-ethylacrylamide in supercritical carbon dioxide, Macromolecules 38 (2005) 2180-2190.
[12] J.K. Kim, I.H. Kim, Characteristics of surface wettability and hydrophobicity and recovery ability of EPDM rubber and silicone rubber for polymer insulators, Journal of Applied Polymer Science 79 (2001) 2251-2257.
[13] A. Labena, K.I. Kabel, R.K. Farag, One-pot synthesize of dendritic hyperbranched PAMAM and assessment as a broad spectrum antimicrobial agent and anti-biofilm, Materials Science and Engineering: C 58 (2016) 1150-1159.
[14] K.I. Kabel, A. Labena, M. Keshawy, W.N. Hozzein, Progressive applications of hyperbranched polymer based on diarylamine: antimicrobial, anti-biofilm and anti-aerobic corrosion, Materials 13 (2020) 2076.
[15] W. Yuan, G. Jiang, J. Che, X. Qi, R. Xu, M.W. Chang, Y. Chen, S.Y. Lim, J. Dai, M.B. Chan-Park, Deposition of silver nanoparticles on multiwalled carbon nanotubes grafted with hyperbranched poly (amidoamine) and their antimicrobial effects, The Journal of Physical Chemistry C 112 (2008) 18754-18759.
[16] G. Zhang, R. Cheng, J. Yan, Y. Xiao, C. Zang, Y. Zhang, Photodegradation property and antimicrobial activity of zinc oxide nanorod-coated polypropylene nonwoven fabric, Polymer Testing 100 (2021) 107235.
[17] M. Avella, M. Errico, S. Martelli, E. Martuscelli, Preparation methodologies of polymer matrix nanocomposites, Applied Organometallic Chemistry 15 (2001) 435-439.
[18] F. Rahma, S. Fellahi, Performance evaluation of synthesized acrylic acid grafted polypropylene within CaCO3/polypropylene composites, Polymer Composites 21 (2000) 175-186.
[19] W. Wu, T. He, J.-f. Chen, X. Zhang, Y. Chen, Study on in situ preparation of nano calcium carbonate/PMMA composite particles, Materials Letters 60 (2006) 2410-2415.
[20]R. K. Farag, A. Labena, S. H. Fakhry, G. Safwat, A. Diab, A. M. Atta, Antimicrobial activity of hybrids terpolymers based on magnetite hydrogel nanocomposites, Materials, (2019); 3604.
[21] M. Okazaki, M. Murota, Y. Kawaguchi, N. Tsubokawa, Curing of epoxy resin by ultrafine silica modified by grafting of hyperbranchedpolyamidoamine using dendrimer synthesis methodology, Journal of Applied Polymer Science 80 (2001) 573-579.
[22] D.M. Xu, K.D. Zhang, X.L. Zhu, Curing of DGEBA epoxy resin by low generation amino-group-terminated dendrimers, Journal of Applied Polymer Science 101 (2006) 3902-3906.
[23] J. Wan, H. Fan, B.-G. Li, C.-J. Xu, Z.-Y. Bu, Synthesis and nonisothermal reaction of a novel acrylonitrile-capped poly (propyleneimine) dendrimer with epoxy resin, Journal of Thermal Analysis and Calorimetry 103 (2011) 685-692.
[24] S. Iraninasab, A. Homaei, E. Mosaddegh, M. Torkzadeh-Mahani, PolyamidoamineDendrimers Functionalized with ZnO-Chitosan Nanoparticles as an Efficient Surface for L-asparaginase Immobilization, Applied Biochemistry and Biotechnology (2023) 1-21.
[25] K. Kabel, A. Labena, W. Gado, Novel, low cost and fast detection sensor for biogenic H_2S gas based on polyaniline/ZnO, CdO and CeO2 nanocomposites at room temperature, Egyptian Journal of Chemistry 64 (2021) 3093-3104.
[26] B. Krishnakumar, T. Imae, Chemically modified novel PAMAM-ZnOnanocomposite: synthesis, characterization and photocatalytic activity, Applied Catalysis A: General 486 (2014) 170-175.
[27] S. Deans, G. Ritchie, Antibacterial properties of plant essential oils, International Journal of Food Microbiology 5 (1987) 165-180.
[28] I. Wiegand, K. Hilpert, R.E.W. Hancock, Agar and broth dilution methods to determine the minimal inhibitory concentration (MIC) of antimicrobial substances, Nature Protocols 3 (2008) 163-175.
[29] D. Amsterdam, Susceptibility testing of antimicrobials in liquid media, Antibiotics in Laboratory Medicine (1996) 52-111.
[30] A.L. Barry, An overview of the Clinical and Laboratory Standards Institute (CLSI) and its impact on antimicrobial susceptibility tests, Antimicrobial Susceptibility Testing Protocols 1 (2007).
[31] A.W. Fothergill, Antifungal susceptibility testing: clinical laboratory and standards institute (CLSI) methods, Interactions of yeasts, moulds, and antifungal agents: How to detect resistance, Springer2011, pp. 65-74.
[32] K. Kumar, P. Giribhattanavar, C. Sagar, S. Patil, A rapid and simple resazurin assay to detect minimum inhibitory concentrations of first-line drugs for Mycobacterium tuberculosis isolated from cerebrospinal fluid, Journal of Global Antimicrobial Resistance 12 (2018) 157-161.
[33] Y. Rukayadi, S. Han, D. Yong, J.-K. Hwang, In vitro antibacterial activity of panduratin A against *Enterococci* clinical isolates, Biological and Pharmaceutical Bulletin 33 (2010) 1489-1493.
[34] S. Modrow, D. Falke, U. Truyen, H.Schätzl, Molecular Virology; Springer: Berlin/Heidelberg, Germany, 2013.
[35] A. Labena, M.A. Hegazy, R.M. Sami, W.N. Hozzein, Multiple applications of a novel cationic gemini surfactant: anti-microbial, anti-biofilm, biocide, salinity corrosion inhibitor, and biofilm dispersion (Part II), Molecules 25 (2020) 1348.
[36] E. Hamzah, M. Hussain, Z. Ibrahim, A. Abdolahi, Influence of *Pseudomonas aeruginosa* bacteria on corrosion resistance of 304 stainless steel, Corrosion Engineering, Science and Technology 48 (2013) 116-120.
[37] M.A. Quraishi, F.A. Ansari, D. Jamal, Thiourea derivatives as corrosion inhibitors for mild steel in formic acid, Materials Chemistry and Physics 77 (2003) 687-690.
[38] J.R. Postgate, The sulphate-reducing bacteria, CUP Archive1979.

[39] A. Ben-David, C.E. Davidson, Estimation method for serial dilution experiments, Journal of Microbiological Methods 107 (2014) 214-221.
[40] L.S. Clesceri, Standard methods for examination of water and wastewater, American public health association 9 (1998) 9–51.
[41] T.L. Miller, M.J. Wolin, A Serum Bottle Modification of the Hungate Technique for Cultivating Obligate Anaerobes, Applied Microbiology 27 (1974) 985-987.
[42] K. Winnicka, M. Wroblewska, P. Wieczorek, P.T. Sacha, E.A. Tryniszewska, The Effect of PAMAM Dendrimers on the Antibacterial Activity of Antibiotics with Different Water Solubility, Molecules 18 (2013) 8607-8617.
[43] S. Alfei, A.M. Schito, Positively charged polymers as promising devices against multidrug resistant Gram-negative bacteria: A review, Polymers 12 (2020) 1195.
[44] B. Rasines, J.M. Hernández-Ros, N. de las Cuevas, J.L. Copa-Patiño, J. Soliveri, M.A. Munoz-Fernandez, R. Gómez, F.J. de la Mata, Water-stable ammonium-terminated carbosilanedendrimers as efficient antibacterial agents, Dalton Transactions (2009) 8704-8713.
[45] E.-R. Kenawy, S. Worley, R. Broughton, The chemistry and applications of antimicrobial polymers: a state-of-the-art review, Biomacromolecules 8 (2007) 1359-1384.
[46] Z. Zaidi, K. Vaghasiya, A. Vijay, M. Sharma, R.K. Verma, S. Vaidya, Hollow ZnO from assembly of nanoparticles: photocatalytic and antibacterial activity, Journal of Materials Science 53 (2018) 14964-14974.
[47] S.R. Meyers, F.S. Juhn, A.P. Griset, N.R. Luman, M.W. Grinstaff, Anionic amphiphilicdendrimers as antibacterial agents, Journal of the American Chemical Society 130 (2008) 14444-14445.
[48] L. Zhang, D. Pornpattananangkul, C.-M. Hu, C.-M. Huang, Development of nanoparticles for antimicrobial drug delivery, Current Medicinal Chemistry 17 (2010) 585-594.
[49] E.R. Gillies, J.M. Frechet, Dendrimers and dendritic polymers in drug delivery, Drug Discovery Today 10 (2005) 35-43.
[50] M.K. Calabretta, A. Kumar, A.M. McDermott, C. Cai, Antibacterial activities of poly (amidoamine) dendrimers terminated with amino and poly (ethylene glycol) groups, Biomacromolecules 8 (2007) 1807-1811.
[51] M. El-Sayed, M. Ginski, C. Rhodes, H. Ghandehari, Transepithelial transport of poly(amidoamine) dendrimers across Caco-2 cell monolayers, Journal of Controlled Release 81 (2002) 355-365.
[52] L. Yang, T.M. Weiss, R.I. Lehrer, H.W. Huang, Crystallization of antimicrobial pores in membranes: magainin and protegrin, Biophysical Journal 79 (2000) 2002-2009.
[53] A.M. Holmes, J.R. Heylings, K.-W. Wan, G.P. Moss, Antimicrobial efficacy and mechanism of action of poly(amidoamine) (PAMAM) dendrimers against opportunistic pathogens, International Journal of Antimicrobial Agents 53 (2019) 500-507.
[54] P. Ortega, J.L. Copa-Patiño, M.a.A. Muñoz-Fernandez, J. Soliveri, R. Gomez, F.J. de la Mata, Amine and ammonium functionalization of chloromethylsilane-ended dendrimers. Antimicrobial activity studies, Organic & Biomolecular Chemistry 6 (2008) 3264-3269.
[55] L. Balogh, D.R. Swanson, D.A. Tomalia, G.L. Hagnauer, A.T. McManus, Dendrimer– silver complexes and nanocomposites as antimicrobial agents, Nano Letters 1 (2001) 18-21.
[56] K. Winnicka, M. Wroblewska, P. Wieczorek, P.T. Sacha, E. Tryniszewska, Hydrogel of ketoconazole and PAMAM dendrimers: Formulation and antifungal activity, Molecules 17 (2012) 4612-4624.
[57] J. Janiszewska, M. Sowińska, A. Rajnisz, J. Solecka, I. Łącka, S. Milewski, Z. Urbańczyk-Lipkowska, Novel dendrimericlipopeptides with antifungal activity, Bioorganic &Medicinal Chemistry Letters 22 (2012) 1388-1393.
[58] D. Byarugaba, Antimicrobial resistance in developing countries and responsible risk factors, International Journal of Antimicrobial Agents 24 (2004) 105-110.
[59] H. Jiang, H. Wang, X. Wang, Facile and mild preparation of fluorescent ZnOnanosheets and their bioimaging applications, Applied Surface Science 257 (2011) 6991-6995.
[60] N.A. Rosli, Y.H. Teow, E. Mahmoudi, Current approaches for the exploration of antimicrobial activities of nanoparticles, Science and technology of advanced materials 22 (2021) 885-907.
[61] M. Li, G. Li, J. Jiang, Z. Zhang, X. Dai, K. Mai, Ultraviolet resistance and antimicrobial properties of ZnO in the polypropylene materials: a review, Journal of Materials Science & Technology 31 (2015) 331-339.
[62] H.-C. Flemming, P.S. Murthy, R. Venkatesan, K. Cooksey, Marine and industrial biofouling, Springer2009.
[63] F.M. Sani, B. Brown, Z. Belarbi, S. Nesic, An experimental investigation on the effect of salt concentration on uniform CO_2corrosion, NACECorrosion, NACE, 2019, pp. NACE-2019-13026.
[64] R. Jia, T. Unsal, D. Xu, Y. Lekbach, T. Gu, Microbiologically influenced corrosion and current mitigation strategies: a state of the art review, International Biodeterioration &Biodegradation 137 (2019) 42-58.
[65] M.S. Suma, R. Basheer, B.R. Sreelekshmy, V. Vipinlal, M.A. Sha, P. Jineesh, A. Krishnan, S.R. Archana, V.S. Saji, S.M.A. Shibli, *Pseudomonas putida* RSS biopassivation of mild steel for long term corrosion inhibition, International Biodeterioration & Biodegradation 137 (2019) 59-67.
[66] N. Kip, J.A. Van Veen, The dual role of microbes in corrosion, The ISME Journal 9 (2015) 542-551.
[67] A. Jayaraman, J. Earthman, T. Wood, Corrosion inhibition by aerobic biofilms on SAE 1018 steel, Applied Microbiology and Biotechnology 47 (1997) 62-68.
[68] L. Daniels, N. Belay, B.S. Rajagopal, P.J. Weimer, Bacterial methanogenesis and growth

from CO_2 with elemental iron as the sole source of electrons, Science 237 (1987) 509-511.
[69] C. Von Wolzgogen, L. van der Klught, Graphication of cast Iron as an Electrochemcialprocess in anaerobic soils, Water, (1934), pp. 147–165.
[70] R. Jia, J.L. Tan, P. Jin, D.J. Blackwood, D. Xu, T. Gu, Effects of biogenic H_2S on the microbiologically influenced corrosion of C1018 carbon steel by sulfate reducing *Desulfovibrio vulgaris* biofilm, Corrosion Science 130 (2018) 1-11.
[71] P. Zhang, D. Xu, Y. Li, K. Yang, T. Gu, Electron mediators accelerate the microbiologically influenced corrosion of 304 stainless steel by the *Desulfovibrio vulgaris* biofilm, Bioelectrochemistry 101 (2015) 14-21.
[72] W. Hamilton, Microbially influenced corrosion as a model system for the study of metal microbe interactions: a unifying electron transfer hypothesis, Biofouling 19 (2003) 65-76.
[73] H. Li, D. Xu, Y. Li, H. Feng, Z. Liu, X. Li, T. Gu, K. Yang, Extracellular electron transfer is a bottleneck in the microbiologically influenced corrosion of C1018 carbon steel by the biofilm of sulfate-reducing bacterium *Desulfovibrio vulgaris*, PloS one 10 (2015) e0136183.
[74] Y. Li, D. Xu, C. Chen, X. Li, R. Jia, D. Zhang, W. Sand, F. Wang, T. Gu, Anaerobic microbiologically influenced corrosion mechanisms interpreted using bioenergetics and bioelectrochemistry: a review, Journal of Materials Science & Technology 34 (2018) 1713-1718.
[75] I. Grabchev, E. Vasileva-Tonkova, D. Staneva, P. Bosch, R. Kukeva, R. Stoyanova, Impact of Cu (II) and Zn (II) ions on the functional properties of new PAMAM metallodendrimers, New Journal of Chemistry 42 (2018) 7853-7862.
[76] K.I. Kabel, L. Kamel, R. Abou-Shahaba, A.E. El-Shenawy, S. Shahen, Some water-soluble polymers as corrosion inhibitors for carbon steel in acidic medium, Al-Azhar Bulletin of Science 28 (2017) 1-10.
[77]K. Khaled, A. Atta, N. Abdel-Shafi, A structure/function study of polyamidoaminedendrimer as a steel corrosion inhibitor, Adsorption 5(3) (2014) 831-840.